Acta metall. Vol. 30, pp. 775 to 784, 1982
Printed in Great Britain

0001-6160/82/040775-10$03.00/0
Pergamon Press Ltd

BAINITE: AN ATOM-PROBE STUDY OF THE INCOMPLETE REACTION PHENOMENON

H. K. D. H. BHADESHIA and A. R. WAUGH

University of Cambridge, Department of Metallurgy and Materials Science, Pembroke Street, Cambridge CB2 3QZ, U.K.

(*Received* 2 *July* 1981; *in revised form* 23 *October* 1981)

Abstract—An imaging atom-probe combined with a high mass-resolution energy-compensated time-of-flight spectrometer has been used to study localised composition changes at the interfaces whose motion leads to the formation of bainite in steels. "Bulk" compositional analysis of the retained austenite and bainitic-ferrite has also been carried out, and the results are interpreted in terms of a new thermodynamic analysis, which allows better distinction between diffusion-controlled growth involving the formation of bainitic-ferrite with a partial supersaturation of carbon, and that in which the ferrite grows with the precise composition of the parent austenite (i.e. in essence martensitic). The fine scale distribution of substitutional alloying elements (Si, Mn) has also been examined. It is believed that the results can be best understood in terms of the martensitic growth of bainite sub-units.

Résumé—Nous avons utilisé une sonde atomique associée à un spectromètre à temps de vol compensé en énergie et à grande résolution en masse afin d'étudier des changements de composition locaux sur les interfaces dont le déplacement conduit à la formation de la bainite dans les aciers. Nous avons également analysé la composition dans la masse de l'austénite résiduelle et de la ferrite bainitique; ces résultats sont analysés à l'aide d'un nouveau modèle thermodynamique qui permet mieux de distinguer entre une croissance contrôlée par diffusion qui conduit à la formation de ferrite bainitique avec une sursaturation partielle de carbone et une croissance au cours de laquelle la ferrite croît avec la composition précise de l'austénite mère (c'est à dire d'essence martensitique). Nous avons également examiné la répartition à petite échelle des éléments d'alliages (Si, Mn) en substitution. Ces résultats s'expliquent á partir de la croissance martensitique de sous unités bainitiques.

Zusammenfassung—Lokale Änderungen der Zusammensetzung wurden an Grenzflächen, deren Bewegung zur Bainitbildung in Stählen führt, mit einer abbildenden Ionensonde, die mit einem energiekompensierten Flugzeitspektrometer hoher Massenauflösung gekoppelt war, untersucht. Außerdem wurde die Zusammensetzung hinsichtlich des Restaustenits und des bainitischen Ferrits im Volumen untersucht. Die Ergebnisse werden mit einer neuen thermodynamischen Analyse gedeutet. Diese Analyse ermöglicht eine verbesserte Unterscheidung zwischen dem diffusionskontrollierten Wachstums einschließlich der Bildung des bainitischen Ferrits mit teilweiser Kohlenstoff-Übersättigung, und dem Fall, in demder Ferrit mit der exakten Zusammensetzung des Mutter-Austenits (d.h. im wesentlichen martensitisch) wächst. Die Feinverteilung der substitutionellen Legierungselemente (Si, Mn) wurde außerdem ermittelt. Es wird angenommen, daß die Ergebnisse am besten erklärt werden können, wenn bainitische Untereinheiten martensitisch wachsen.

INTRODUCTION

One of the outstanding problems associated with the study of transformations in steels is the determination of the carbon content of *freshly formed* bainitic ferrite. The difficulty arises because direct experimental measurements can only focus on the post-transformation composition, which need not correspond to that existing during growth itself. In particular, any carbon supersaturation in the ferrite can be relieved either by the precipitation of carbides within the ferrite, or by the partitioning of carbon into the residual austenite by means of diffusion. Both these processes can be very rapid, because of the high mobility of carbon in iron, especially at the temperatures where bainite forms. These interfering reactions usually occur simultaneously, but it is possible to suppress cementite precipitation by the judicious use of silicon as an alloying element [1]. On the other hand, the rejection of excess carbon into residual austenite seems inevitable (especially at the relatively high temperatures involved), making a direct determination of the carbon content of bainitic-ferrite impossible.

There is, however, a way in which an indirect solution to this problem can be achieved [2]. Consider the case where bainitic-ferrite inherits the full carbon content of the parent austenite during transformation. The reaction should, in principle, go to completion since there is no diffusion necessary. In practice, the whole of the austenite grain does not transform instantaneously because of kinetic restrictions (e.g. heterogeneous nucleation); even if the first plate of bainite forms with full supersaturation, it has an *opportunity* to reject its excess carbon into the remaining austenite. Any further increment of transformation is

therefore associated with a lower free energy change, due to the higher carbon content of the austenite from which it has to form. Eventually, a stage is reached where transformation becomes thermodynamically impossible† since the free energies of the residual austenite and the bainitic-ferrite (of the same composition) become identical. Hence, by monitoring the stage at which the bainite transformation stops, it should be possible to deduce the level of carbon supersaturation in ferrite *during* growth. The formation of fully supersaturated bainite requires the carbon content of the austenite to fall below that indicated by the T_0' curve. A less than full supersaturation would lead to transformation conditions *closer* to equilibrium and a correspondingly increased maximum possible degree of transformation; the terminal carbon content of the austenite would also be higher, and nearer to that given by the extrapolated *Ae3'*phase boundary.

Bhadeshia and Edmonds [2, 3] measured the extent of transformation at the point where the bainite reaction ceases, and found that this approximately conformed with the T_0 line, but was in considerable disagreement with the *Ae3'* (or *Ae3''*) composition (this effect is known as the *incomplete-reaction phenomenon*), implying that bainite does indeed grow with a supersaturation of carbon. They pointed out that exact agreement with the T_0 line (or indeed with the T_0' line) cannot be expected since the distribution of carbon in the austenite was not uniform (the reasons for this are detailed in Refs [2–5]); this should lead to a greater than expected volume fraction of transformation even if bainite formation involved full carbon supersaturation. It is also pertinent to emphasize that it is experimentally difficult to distinguish between the T_0 and T_0' lines (which differ only because the latter accounts for the stored energy of bainite) since favourable strain interactions between sheaves of bainite combined with plastic relaxation effects make the value of the stored energy uncertain.

It is clear that the existence of an inhomogeneous distribution of carbon is an important factor in the development of the bainite transformation, and Bhadeshia and Edmonds [2] offered metallographic evidence to this effect. Self *et al.* [4] subsequently proved quantitatively the existence of non-uniform distributions of carbon in the austenite retained after bainitic transformation, using a high-resolution lattice imaging technique. In the present work, an (imaging) atom-probe is used to provide further *direct* quantitative proof for the irregular distribution of carbon, on an ultra-high resolution scale. The results of the atom-probe experiments have also been subjected to a new kind of a thermodynamic analysis, in order to facilitate distinction between bainite transformation involving *some* partitioning of carbon during growth, and that which is in essence martensitic. It should be noted that all the other techniques used to date are indirect, and rely on various calibration procedures, and can be sensitive to imaging conditions and instrumental aberrations.

† The locus of such positions, as a function of isothermal transformation temperature defines the T_0' curve, where austenite and bainite (with a certain amount of stored energy associated with transformation strains) of the same composition have equal free energies. The corresponding curve for stress-free austenite and ferrite of identical composition is conventionally called the T_0 curve. The *Ae3''* and *Ae3'* (the former accounting for the stored energy of the ferrite) curves may be similarly defined for growth involving the paraequilibrium partitioning of carbon (but not of substitutional alloying elements). For plain carbon steels, it follows that the *Ae3'* and *Ae3* curves are identical.

EXPERIMENTAL PROCEDURES

The experimental alloy was prepared from high-purity base materials as a 20 kg vacuum induction melt. The ingot was forged and hot-rolled to 10 mm diameter rod followed by a hot-swage reduction to 8 mm diameter rod. After removing 2 mm from the surface, a 60 g piece of the alloy was sealed in a quartz capsule under a partial pressure of argon and homogenized at 1250°C for a period of 3 days before water quenching. The final composition of the alloy was (wt. %) Fe–0.43 C–2.02 Si–3.0 Mn. The alloy was then resealed, austenitised at 1200°C for 10 min and isothermally transformed at 350°C in a molten-tin bath (for 10 h), followed by a water quench. This heat-treatment ensures that the bainite reaction proceeds to its maximum extent consistent with the incomplete-reaction phenomenon discussed above (Refs [2–5]).

Field-ion specimens (0.5 × 0.5 × 20 mm square section rods) were precision machined from the *single* heat-treated sample, under conditions of flood lubrication (the results thus refer to different areas of the same specimen; the different areas were physically obtained by using different rods, or by repolishing the same rod). A length of one of the ends of each specimen was then coated with a proprietary lacquer, and partially submerged into an electrolyte of 10% perchloric acid in acetic acid; electropolishing (20–25 V) was carried out at room temperature to produce a necked region which was then electropolished (15V d.c.) in a 2% perchloric acid/2-butoxyethanol mixture, until the specimen parted at the neck. Electropolishing was briefly continued beyond this stage in order to remove any deformed region.

An imaging atom-probe combined with a high mass-resolution energy-compensated time-of-flight spectrometer (the instrument is described in Ref. [6]) was used, not only to obtain direct compositional analysis, but also to map the distribution of alloying elements on an ultra-fine scale. During analysis, the background pressure was maintained at less than 1.2×10^{-7} Pa; the specimen cryostat was cooled with solid nitrogen. The pulse-repetition rate was 220 Hz, and ion collection rates (through an effective probe hole of ~3 nm) of between 10^{-2} and 10^{-3} ions per pulse were used to ensure that each detection event

corresponded to just one ion. A neon gas pressure of 0.01 Pa was used for imaging purposes. The magnitude of the pulse factor was always maintained within the range 15–20%, in order to ensure that it did not effect any of the measured concentrations.

RESULTS AND DISCUSSION

The development and detailed nature of the microstructure obtained after heat-treatment has been discussed elsewhere [3, 5], but a typical electron micrograph showing a sheaf of bainite is presented in Fig. 1a. The sheaf consists of platelets of bainitic-ferrite, of identical orientation in space, separated by carbon-enriched films of retained austenite. In fact, crystallographic variants of sheaves are known to bound relatively larger islands of retained austenite [7], but these could not be studied in the present experiments; these islands have been shown to contain less carbon than the film morphology of austenite, and are certainly less stable to martensitic transformation. In the environment of the field-ion microscope, they tended to lead to catastrophic specimen failure.

Figure 1b illustrates the calculated T_0, T_0', $Ae3'$ and $Ae3''$ boundaries for the alloy used; the details of the calculations have been given elsewhere (2, 5), but it should be noted that the stored energy of bainite was taken to be 400 J/mole, in accordance with the recent work of Bhadeshia [5].

Quantitative analysis was carried out on some ten specimens, collecting 1000–20,000 (typically 10,000) ions per data point in order to minimise the effects of statistical composition fluctuations. Carbon was observed in the mass-spectra at mass-to-charge ratios of $6(C^{2+})$, $12(C^{+})$, $18(C_3^{2+})$, $24(C_2^{+})$ and $36(C_3^{+})$, as has been noted for other steels (Ref. [6]). Data were taken from the bulk phases as well as across the ferrite-austenite interfaces; the results are presented in Fig. 2, where all points which (within the limits of experimental error) fall above the average carbon content of the alloy ($\bar{x} = 1.93$ at.%) refer to austenite. Only a limited amount of data on the levels of manganese could be obtained because the adjacent manganese and iron isotopes could only be properly resolved under favourable circumstances; these results were found to be consistent with identical concentrations of manganese in ferrite and in austenite.

Growth involving full supersaturation

The results of Fig. 2 clearly demonstrate the non-uniform distribution of carbon in the retained austenite. The carbon concentration in many cases exceeds that given by the T_0' curve (Fig. 1b, 2), although the majority of results fall below the level consistent with the $Ae3''$ calculations. The results can still be interpreted to be in accord with the contention that bainite initially forms with a *full* supersaturation of carbon, despite the apparent disagreement with the T_0' criterion. This becomes clear when it is realised that the austenite can continue to *accumulate* carbon from suitable sources, up to a maximum corresponding to the $Ae3''$ limit, although it cannot then *transform* to fully supersaturated ferrite. A small region of austenite which has already been affected by the dumping of carbon from an extant bainite plate may become isolated by the formation of further supersaturated platelets in close proximity. The subsequent rejection

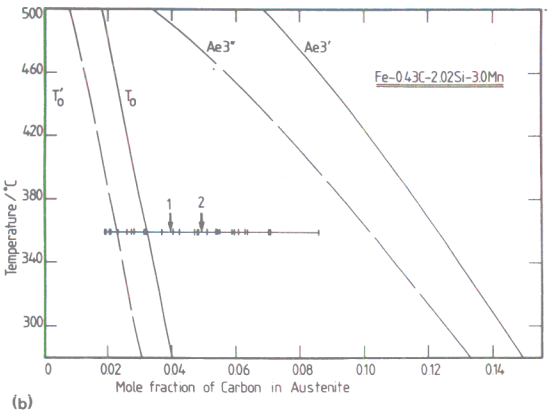

Fig. 1. (a) Electron micrograph showing a typical sheaf of bainite (isothermally transformed at 350°C). The bainite sub-units (lighter colour) are separated by regions of carbon-enriched retained-austenite. (b) Phase diagram for the analysis of the Incomplete-Reaction Phenomenon. The $Ae3'$ and $Ae3''$ curves represent constrained phase equilibria between α and γ, since they relate to reactions in which substitutional alloying elements do not partition. The T_0 and T_0' curves represent partitionless transformation. The dashed curves differ from the corresponding continuous curves in that they allow for the stored energy of ferrite. Experimental determinations of the carbon content of austenite (x_γ) are also included, but are better presented in Fig. 2. Arrow (1) refers to the maximum x_γ deduced in Ref. [2], and arrow (2) is the mean of the present determinations.

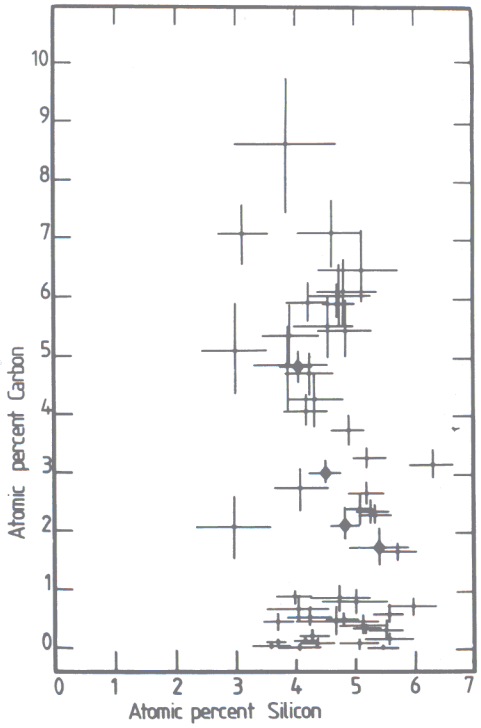

Fig. 2. Atom-probe determinations of the carbon and silicon contents of bainitic-ferrite and retained austenite (the results corresponding to austenite all have a carbon content in excess of the average alloy carbon content, $\bar{x} = 1.93$ at.%). The error bars represent statistical counting errors arising due to the finite number of ions collected. The mean silicon concentration is 4.70 at.%, and compares well with the alloy chemical analysis (3.98 at.%). The diamond shaped points refer to data collected at the austenite-ferrite interface, through a probe hole of ~3 nm diameter.

of carbon from the latter can then raise the carbon content of the entrapped austenite to levels beyond the T_0' curve. The probability of such a sequence of events is high because of the nature of bainite sheaf development [2]. An inhomogeneous distribution of carbon is also to be expected under these circumstances, since the local carbon content of any isolated region of austenite must depend on the state of isolation, the morphology and the exact sequence of transformation.

Growth involving partial supersaturation

An alternative interpretation could arise if bainite growth, at all stages of transformation, involved only a *partial* supersaturation, the remainder being pushed ahead of the transformation interface, giving diffusion controlled kinetics. In other words, it might be assumed that since some of the experimental data (Fig. 1b, 2) falls between the T_0' and $Ae3''$ boundaries, the level of carbon in the ferrite during growth must have been less than $\bar{x}$, although greater than the corresponding equilibrium concentration.†

Referring to Fig. 3, it is possible (see Appendix I) to calculate the interface tie-line compositions for growth involving partial supersaturation. If $\bar{x}$ is the average alloy carbon concentration, the tie-line $x_\alpha^1 - x_\gamma^1$ refers to the formation of bainitic-ferrite with a carbon excess of $(x_\alpha^1 - x_\alpha^{\alpha\gamma})$, with reaction termination occurring when the austenite carbon level reaches x_γ^1. It should be noted that Fig. 3 properly depicts the conditions involved in the present work since $\bar{x}$ falls to the left of the intersection of the alpha and gamma free-energy curves. If the supersaturation in the ferrite is now allowed to approach $\bar{x}$, then x_γ^1 tends towards x_γ^m. In the limit that $x_\alpha^1 = \bar{x}$ we obtain the unexpected result that growth involving partial supersaturation must have a *minimum* terminal carbon level in the austenite, given by x_γ^m. Clearly, an austenite tie-line composition less than x_γ^m (e.g. x_γ^2) is physically unreasonable since it corresponds to a ferrite supersaturation exceeding $\bar{x}$. Calculations were carried out to determine sets of tie-line compositions (i.e. $x_\alpha^I - x_\gamma^I$) over the range $x_\alpha^{\alpha\gamma} < x_\alpha < x^{T_0}$ and $x^{T_0} < x_\gamma < x_\gamma^{\gamma\alpha}$. The results are plotted (as a curve) in Fig. 4; it should be noted that the stored energy of bainite was taken to be 400 J/mole for the purposes of the calculations. The experimentally determined values of x_γ are also plotted in Fig. 4 such that they coincide with the theoretical curve; the average alloy carbon content is represented by a horizontal line.

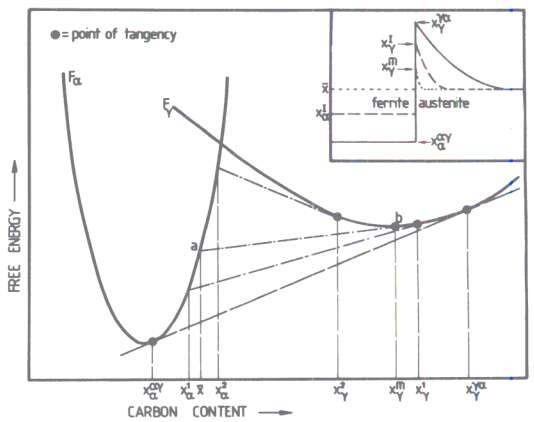

Fig. 3. Schematic free energy curves for the analysis of ferrite growth involving partial-supersaturation, as discussed in the text. The inset illustrates the sort of composition profiles to be expected across the transformation interface, under conditions of steady-state growth, with carbon content and position relative to the interface plotted on the ordinate and abscissa respectively. Lines such as *ab* mark the tie-line compositions involved in diffusion-controlled growth (the general corresponding set of compositions linked by a tie line such as *ab* are labelled x_α^I and x_γ^I).

† We note that since some partitioning of carbon is assumed to occur even at the *beginning* of transformation, the actual level of excess carbon in the ferrite must, at *any* stage of the reaction, be less than or equal to the *initial* level of supersaturation (which is in turn less than $\bar{x}$). This is because the driving force for reaction decreases with the progress of transformation, and it becomes increasingly difficult for the ferrite to maintain the starting level of supersaturation.

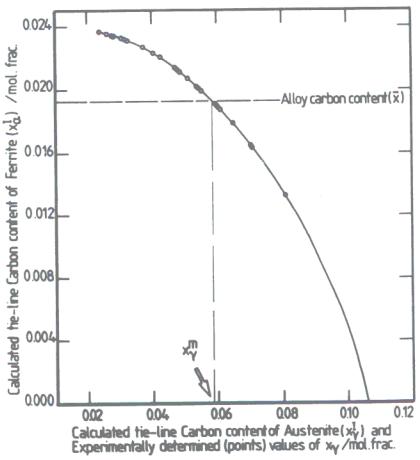

Fig. 4. Graph of x_α^I vs x_γ^I. Each experimental determination of the carbon content of austenite is treated as a value of x_γ^I and is plotted to coincide with the theoretical curve, so that the corresponding level of supersaturation in the ferrite can be inspected.

Figure 4 clearly demonstrates that the calculated levels of supersaturation (corresponding to the *experimental* data) that exist in the ferrite during growth are always very high even if it is assumed that growth is diffusion-controlled; more significantly, it is evident that the majority of the experimental data fall *below* x_γ^m. As deduced earlier, this would imply higher levels of carbon supersaturation in the ferrite than is physically possible, and the results must therefore be taken to be inconsistent with the hypothesis that bainitic-ferrite formation occurs with some partitioning of carbon during growth.

It should be pointed out, that if growth *does* involve the formation of partially supersaturated ferrite, it is not obvious as to why the level of supersaturation should vary as it does. It would also appear that growth under the circumstances of partial supersaturation would be unstable, and should rapidly degenerate to that involving a zero excess of carbon in the ferrite [5].

While it seems reasonable that the hypothesis of ferrite growth involving supersaturations less than $\bar{x} - x_\alpha^{\alpha\gamma}$ can be discounted (for the reasons given above), there is yet a third possible interpretation. In this, the sub-units of bainite may first grow martensitically, with subsequent carbon rejection into the residual austenite, until the carbon content of the latter reaches the T_0' line. At this point, the bainite *could* start growing with a lower carbon content than the now *enriched* remaining austenite (although the level of carbon in the ferrite could exceed $\bar{x}$). However, such an interpretation seems unsatisfactory since there is then no clear reason why the bainitic-ferrite should not *continue* to grow with successively decreasing levels of excess carbon, until reaction stops when the austenite carbon content reaches the *Ae*3″ line. The latter clearly does not occur, and hence it is believed that bainite growth involving full supersaturation (i.e. each sub-unit growing martensitically) is still the most reasonable interpretation of the incomplete-reaction phenomenon, with the apparent discrepancy between the measured austenite carbon contents and the T_0' curves arising due to the incidental kinetic factors mentioned earlier. It should be noted that in considering diffusion-controlled growth, no direct account has been taken of the reduction in available driving force due to capillarity (Gibbs-Thompson) or interface reaction effects. This is because the value of the stored energy (400 J/mole, Ref. [5]) was deduced by calculating the driving force available at the onset of bainite formation, and if growth *is* diffusion-controlled, the stored energy term should include the influence of the above mentioned effects. Judging from the behaviour of Widmanstatten ferrite (Ref. [5]), which is a true diffusion-controlled displacive transformation, such effects should not account for more than about 50 J/mole of driving force.

Other Results

Turning now to the observed *post-transformation* carbon content of bainitic ferrite, the data of Fig. 2 shows significantly higher than equilibrium carbon concentrations. It is believed that this is due to the high dislocation density of bainitic-ferrite; segregation at dislocations might be expected to bind, and hence prevent or hinder the carbon atoms from diffusing out of the ferrite lattice. The results are indicative of an after effect of the high level of carbon that existed in the bainitic ferrite at an early stage of its growth.

Some direct evidence on the distribution of carbon in ferrite was obtained using the atom-probe in its imaging mode. Figure 5 illustrates a case where the segregation of carbon, to what is presumably a highly-dislocated region within the ferrite, is very pronounced.† (Images taken with other species of carbon showed similar effects.) It should be noted that it is the ratio of the image intensities (of say the C and Fe ion images) that reflects concentration levels, rather than absolute intensities in individual images, since the latter may be affected by local magnification variations [6]. It was therefore necessary to take an image with Fe-ions in every case; in quantitative analysis all the ions are automatically taken into account. Imaging atom-probe experiments were also carried out at austenite/bainitic-ferrite interfaces. The quantitative analysis results of Fig. 2 are based on an effective probe hole diameter of ~3 nm, and therefore rep-

† The segregation of carbon to defects clearly results in an overestimation of the general carbon content of the ferrite; atom-probe work is necessarily concerned with extremely localised composition variations and the defect density in both the ferrite and austenite is known to be high [2]. Hence some of the high-carbon ($>\bar{x}$) data may also be an overestimate of the average (on the scale of an isolated region of austenite) composition of the austenite. This is evident from Fig. 1b, which shows that the mean of all the austenite results exceeds the value obtained (Ref. [2]) by measuring the *maximum* amount of transformation to bainite.

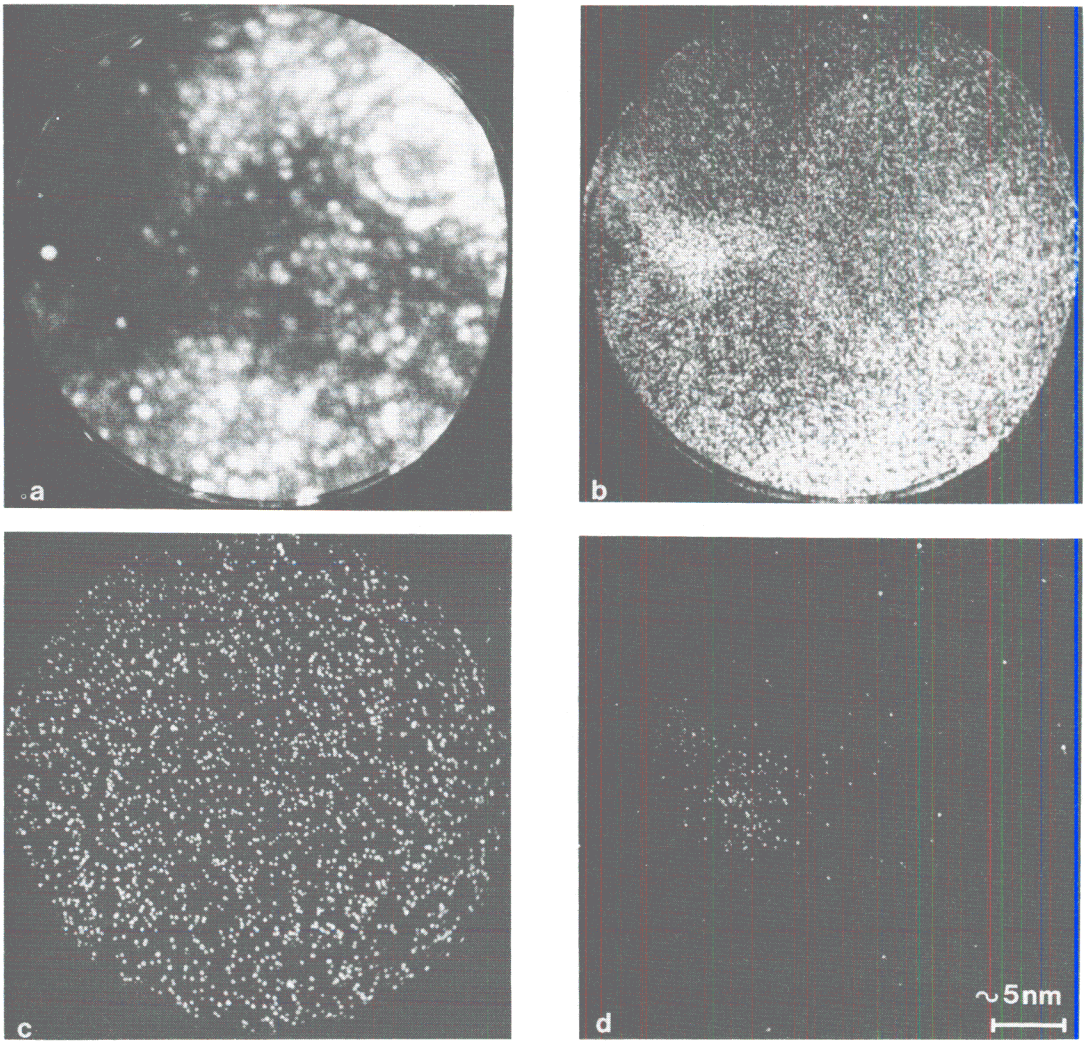

Fig. 5. Imaging atom-probe illustrating the segregation of carbon in ferrite. (a) Field-ion image. (b) Corresponding iron map. (c) Corresponding silicon map. (d) Corresponding carbon map. The carbon concentration in the relatively intense area is 0.88 ± 0.11 at.%. It is believed that this region consists of a number of dislocation terminations, consistent with the relatively higher desorption of iron atoms seen in the same area of the iron desorption image of Fig. 5b.

resent averaged compositional variations, albeit on an ultra-fine scale. This is clearly a limiting factor in the study of segregation to interfaces, and the imaging atom-probe is a powerful qualitative alternative for mapping even more localised compositional fluctuations. From Fig. 6 it is clear that there is no significant segregation of either silicon or carbon to the austenite-ferrite interface; this also implies the absence of any significant manganese segregation, since the latter would lead to perturbations in the silicon image.† The accompanying quantitative data (Fig. 6) confirms the absence of any partitioning of silicon between the phases involved. The results are fully consistent with the fact that an invariant-plane strain shape change accompanies the formation of bainite [8, 9] and with the existence of an atomic correspondence between the austenite and bainitic-ferrite during transformation. The absence of any significant carbon build-up at the interface is surprising at first sight, but it should be noted that the interface involved must be semi-coherent (with a high degree of coherency, consistent with the shape change effect mentioned earlier) and may not provide a very large sink for carbon atoms. This would appear contradictory to recent work [10] which indicates the presence of at least 20 at.% of carbon at the austenite/tempered-martensite interfaces. However, it would not only be difficult to explain such a large degree of

† Manganese segregation would perturb the silicon desorption image since the activity (and hence concentration) of the silicon must depend on that of manganese. It is reasonable to expect, simply on the grounds of thermodynamic stability, that any segregation effects would be coupled, since the activity coefficient of any element is in general a function of the concentration of all the other elements.

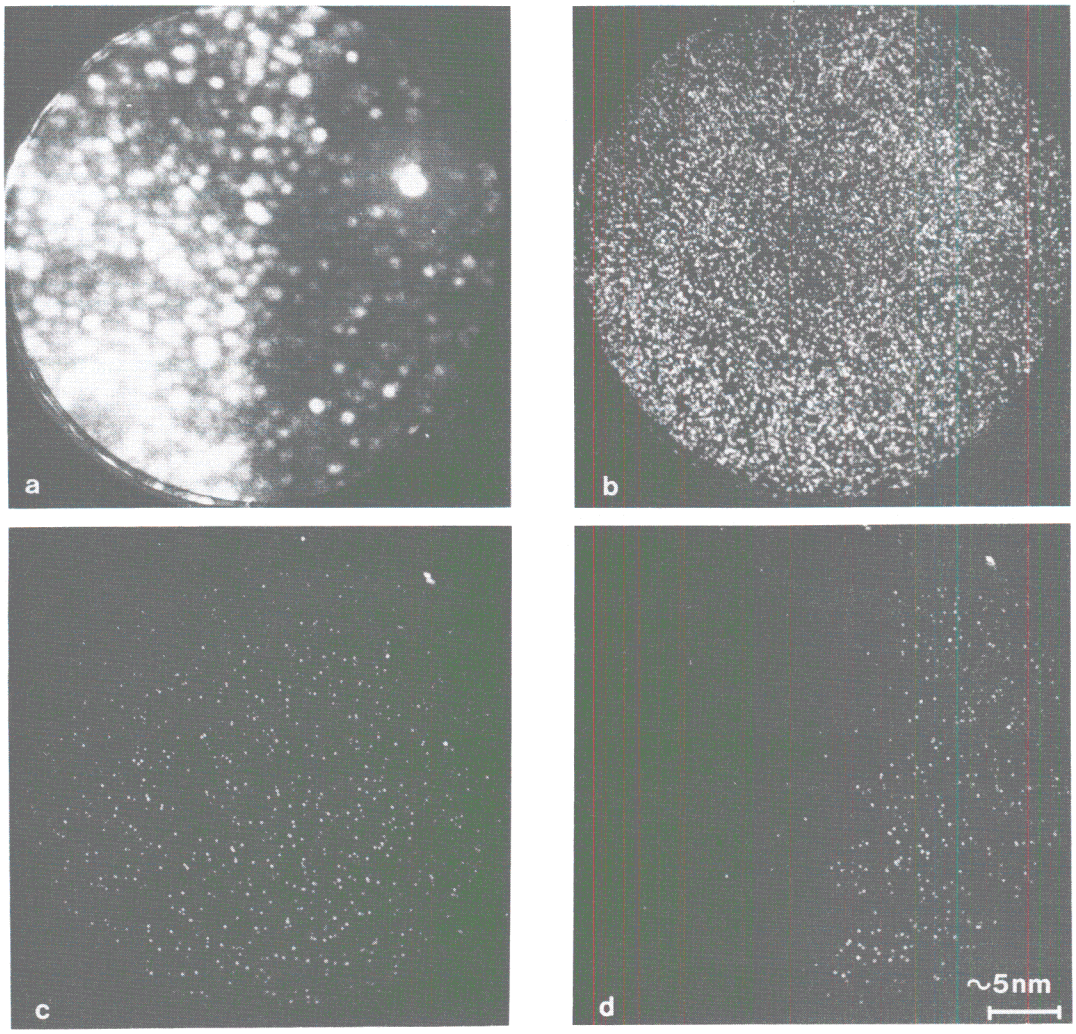

Fig. 6. Imaging atom-probe micrographs, taken across an austenite-bainitic ferrite interface. (a) Field-ion image. (b) Corresponding iron map. (c) Corresponding silicon map. (d) Corresponding carbon map. The corresponding quantitative determinations, made through a probe-hole of ~3 nm diameter, are as follows (at.%):

	Silicon	Carbon
In ferrite, away from interface	4.78 ± 0.68	0.49 ± 0.22
In ferrite, away from interface	5.10 ± 0.51	0.80 ± 0.19
In austenite away from interface	5.12 ± 0.64	6.48 ± 0.72
In austenite away from interface	4.81 ± 0.49	7.12 ± 0.60
In austenite near interface	4.89 ± 0.50	6.13 ± 0.56
Probe hole positioned at interface	4.10 ± 0.20	4.82 ± 0.23

carbon segregation to glissile semi-coherent interfaces, but it is also possible that the experiment concerned [10] could have detected the presence of carbides, arising either from *in-situ* autotempering or from the imposed tempering treatment. The latter interpretation would also be consistent with the large *width* of the carbon profile observed in these particular experiments. In the present experiments, carbide precipitation does not arise, because of the presence of silicon and because of the nature of the heat-treatment used. Additional depth-profiling atom-probe experiments confirming these results are given in Appendix II and in Ref. [11]. It should also be stressed that the imaging atom-probe micrographs discussed above are a representative part of a larger and equivalent set of accumulated results.

GENERAL SUMMARY

The isothermal bainite reaction does not proceed to completion, in the sense that transformation ceases well before the carbon content of the remaining austenite reaches the $Ae3''$ metastable-phase equilibrium boundary. Direct evidence has been obtained to dem-

onstrate the inhomogeneous distribution of carbon in the residual austenite, and the results have been used to deduce the level of carbon that existed in the ferrite, *during* growth. The analysis clearly indicates that very high levels of excess carbon exist in bainitic-ferrite during growth, but there are three main ways of interpreting the results:

(1) The bainite sub-units grow martensitically at all stages of transformation; this seems the most reasonable interpretation and is consistent with the existence of both the inhomogeneous distribution of carbon, and the incomplete reaction phenomenon.

(2) Bainite growth is diffusion-controlled, with the carbon content of the ferrite never exceeding the average alloy composition, although the ferrite may be supersaturated to any other extent. This is inconsistent with the thermodynamics of growth involving partial supersaturation (much of the experimental data fall below x_γ^m), and the question of growth stability remains unresolved, as does the explanation for the variations in the expected levels of supersaturation.

(3) Bainite growth is initially martensitic, but ceases to be so when the carbon content of the austenite (now enriched due to the post-transformation rejection of carbon from the fully supersaturated ferrite) reaches the T_0' boundary. This also suffers from the problems of the previous interpretation, and in addition, it is not obvious why such a sequence of events should not lead (by successive reductions in the level of ferrite supersaturation) to complete reaction, to the extent of the *Ae3″* phase boundary.

Imaging atom-probe and other results indicate the absence of any significant build up of either carbon or substitutional elements to the transformation interface.

Finally, it should be emphasized that the interpretations presented in this paper can only be correct if the incomplete-reaction phenomenon can be attributed largely to the existence of non-equilibrium levels of carbon in the ferrite lattice at the growth stage. However, there do not seem to be any striking alternative ways of interpreting the incomplete-reaction phenomenon; that the latter is not a manifestation of some restriction to diffusional transformation has been demonstrated in earlier work [2, 5], but more extensive results on this particular aspect are in the process of publication.

Acknowledgements—The authors are grateful to the Science Research Council for the provision of research fellowships, and to Professor R. W. K. Honeycombe FRS for the provision of laboratory facilities.

REFERENCES

1. R. F. Hehemann, *Phase Transformations*, p. 397. A.S.M. Metals Park, Ohio (1970).
2. H. K. D. H. Bhadeshia and D. V. Edmonds, *Acta metall.* **28,** 1103 (1980).
3. H. K. D. H. Bhadeshia and D. V. Edmonds, *Metall. Trans.* **10A,** 895 (1979).
4. P. Self, H. K. D. H. Bhadeshia and W. M. Stobbs, *Ultramicroscopy* **6,** 29 (1981).
5. H. K. D. H. Bhadeshia, *Acta metall.* **29,** 1117 (1981).
6. A. R. Waugh and M. J. Southon, *Surface Sci.* **89,** 718 (1979).
7. H. K. D. H. Bhadeshia, Ph.D. Thesis, University of Cambridge (1976).
8. G. R. Speich, *The Decomposition of Austenite by Diffusional Processes*, p. 353. Interscience, New York (1962).
9. G. R. Srinivasan and C. M. Wayman, *Acta metall.* **16,** 609 (1968).
10. S. J. Barnard, G. D. W. Smith, M. Sarikaya and G. Thomas, *Scripta. Metall.* **15,** 387 (1981).
11. H. K. D. H. Bhadeshia and A. R. Waugh, Presented at the International Conference on Solid-Solid Phase Transformations, Pittsburgh (1981).
12. J. W. Christian, *Theory of Transformations in Metals and Alloys*, Part 1, 2nd edn, p. 173. Pergamon Press, Oxford (1975).

APPENDIX I. THERMODYNAMICS OF GROWTH INVOLVING PARTIAL SUPERSATURATION

In the discussion that follows, it is assumed that transformation occurs without the partitioning of any substitutional alloying elements.

In the main text of this paper it was suggested that in circumstances where the growth of partially supersaturated ferrite (level of supersaturation $<\bar{x}$) is diffusion-controlled, there exists a *lower* limit (x_γ^m) to the composition of the austenite at the transformation interface. This limit corresponds to the ferrite interface tie-line composition (x_α^I) equal to the average carbon content of the alloy ($\bar{x}$). Hence, in all cases where some carbon is partitioned during growth, and where $x_\alpha^I \leqslant \bar{x}$, the carbon content of the austenite at reaction termination ($\equiv x_\gamma^I$) must exceed x_γ^m, so that

$$x_\gamma^m \leqslant x_\gamma^I \leqslant x_\gamma^{\gamma\alpha} \quad \text{and} \quad x_\alpha^{\alpha\gamma} \leqslant x_a^I \leqslant \bar{x}.$$

In Fig. 3, the free energy (F) is plotted against the carbon content (x) of the phase concerned. The equation describing the tangent ab is given by (see Ref. [12])

$$F_{\text{tangent}} = (1 - x)(\overline{F}_{\text{Fe}}^\gamma) + x(\overline{F}_{\text{C}}^\gamma) \qquad \text{(A1)}$$

where $\overline{F}_{\text{Fe}}^\gamma$ and $\overline{F}_{\text{C}}^\gamma$ refer to the partial molar free energies of iron and carbon (both in the austenite phase), *for austenite of composition* $x_\gamma = x_\gamma^m$ (both the partial molar free energies are obviously composition dependent).

Equation 1 may be expanded as

$$F_{\text{tangent}} = (1 - x)[F_{\text{Fe}}^{0\gamma} + RT\ln|a_{\text{Fe}}^\gamma\{1 - x_\gamma^m\}|] + x[F_{\text{C}}^{0\text{G}} + RT\ln|a_{\text{C}}^\gamma\{x_\gamma^m\}|] \qquad \text{(A2)}$$

where $F_{\text{Fe}}^{0\gamma}$ and $F_{\text{C}}^{0\text{G}}$ are the free energies of the pure components referred to austenite and to pure graphite as the standard states, and the terms in the curly brackets are arguments of the corresponding activity functions (a = activity, R = constant, T = absolute temperature).

The free energy of ferrite (F_α) of composition x may be similarly represented as

$$F_\alpha = (1 - x)[F_{\text{Fe}}^{0\alpha} + RT\ln|a_{\text{Fe}}^\alpha\{1 - x\}|] + x[F_{\text{C}}^{0\text{G}} + RT\ln|a_{\text{C}}^\alpha\{x\}|]. \qquad \text{(A3)}$$

For the point of intersection of the tangent ab with the F_α curve, (i.e. $x = \bar{x}$), equations A2 and A3 may be

equated to give

$$(1-\bar{x})\left[\Delta F_{Fe}^{\gamma\to\alpha}+RT\ln\left|\frac{a_{Fe}^{\alpha}\{1-\bar{x}\}}{a_{Fe}^{\gamma}\{1-x_{\gamma}^{m}\}}\right|\right]+\bar{x}\left[RT\ln\left|\frac{a_{C}^{\alpha}\{\bar{x}\}}{a_{C}^{\gamma}\{x_{\gamma}^{m}\}}\right|\right]=0 \qquad (4)$$

where $\Delta F_{Fe}^{\gamma\to\alpha}$ is the free energy change accompanying transformation in pure iron. Equation 4 can be solved iteratively for $\bar{x}$, given x_{γ}^{m}, or vice versa.

The thermodynamic data necessary for this has been discussed elsewhere [2, 5], but we note that stored energy can be accounted for by modifying the $\Delta F_{Fe}^{\gamma\to\alpha}$ term.

APPENDIX II. SEQUENTIAL DATA AND FURTHER EXPERIMENTAL RESULTS

The data collected from an atom probe in a field-evaporation sequence yields information on both the *average* composition, and the detailed *spatial distribution* of the alloying elements in the phase concerned. Figures AII.1 and AII.2 illustrate the results of separate field-evaporation experiments, carried out on isolated regions of ferrite and of austenite, respectively. The data are plotted as concentrations averaged over 400 ions (changing this to 100 or 200 did not alter the form of any of the curves presented, but simply increased the noise levels), versus the total number of ions collected. The specimens used in these experiments were from the same sample as used in the work presented in the main text of this paper.

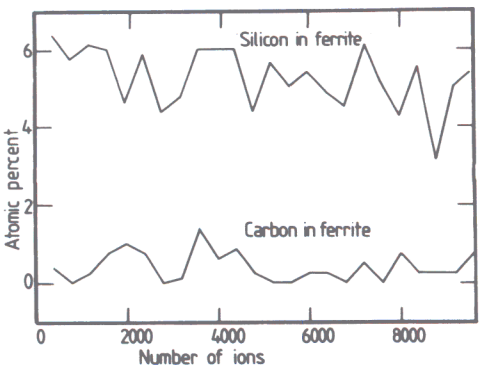

Fig. AII.1. Field evaporation sequence showing the distribution of carbon and silicon in bainite ferrite (Fe–Mn–Si–C alloy).

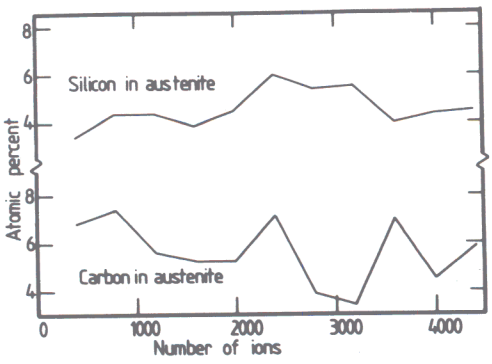

Fig. AII.2. Field evaporation sequence showing the distribution of carbon and silicon in austenite (Fe–Mn–Si–C alloy).

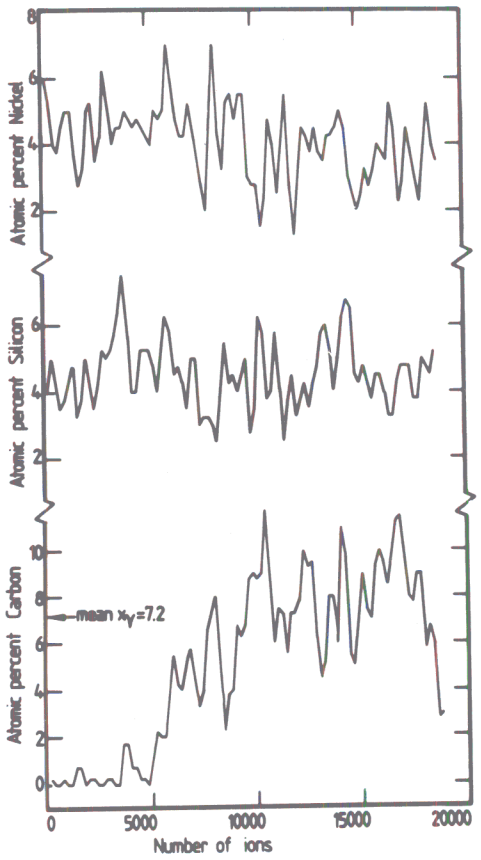

Fig. AII.3. Field evaporation sequence, traversing a bainitic-ferrite/austenite interface (Fe–Ni–Si–C alloy).

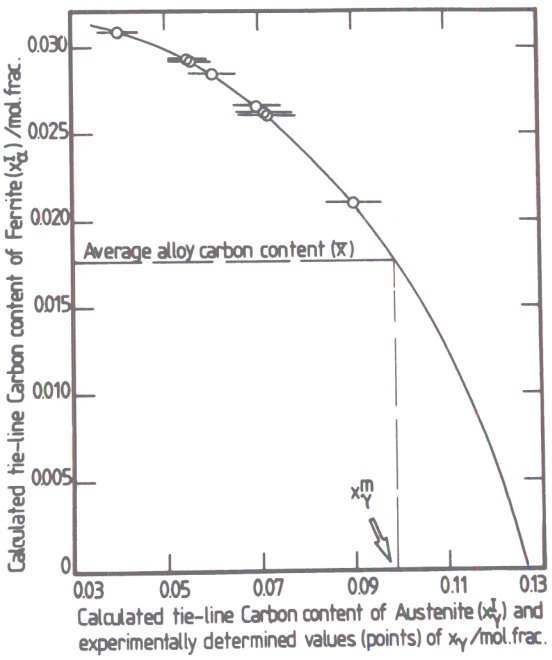

Fig. AII.4. Fe–0.39 C–2.05 Si–4.08 Ni wt.% alloy isothermally transformed at 340°C. Graph of x_{α}^{I} vs x_{γ}^{I}. Each experimental determination of the carbon content of austenite is treated as a value of x_{γ}^{I} and is plotted to coincide with the theoretical curve, so that the corresponding level of supersaturation in the ferrite can be inspected.

Experiments were also carried out on a Fe–0.39 C–2.05 Si–4.08 Ni wt% alloy, isothermally transformed at 340°C for 10 h after austenitising at 1100°C for 15 min, to give (on reaction termination) a microstructure of bainitic-ferrite and carbon-enriched retained austenite. The results of a field evaporation sequence *through* a ferrite/austenite interface are presented in Fig. AII.3. As expected, these data (and those of Figs AII.1,2) show that substitutional elements do not redistribute during the bainite transformation. It is also evident that there is no significant segregation of any of the alloying elements at the position of the interface, in agreement with the detailed quantitative and imaging atom-probe experiments presented in the main text.

Figure AII.4 illustrates results on the carbon content of the austenite in the Fe–Ni–Si–C steel; this figure is directly comparable to Fig. 4, and does not require further explanation. It is clear that the carbon content of the austenite remains below x_γ^m, providing further support for the conclusions presented earlier.